

Inhibition of Mutant α B Crystallin-Induced Protein Aggregation by a Molecular Tweezer

Na Xu, PhD; Gal Bitan, PhD; Thomas Schrader, PhD; Frank-Gerrit Klärner, PhD; Hanna Osinska, PhD; Jeffrey Robbins, PhD

Background—Compromised protein quality control causes the accumulation of misfolded proteins and intracellular aggregates, contributing to cardiac disease and heart failure. The development of therapeutics directed at proteotoxicity-based pathology in heart disease is just beginning. The molecular tweezer CLR01 is a broad-spectrum inhibitor of abnormal self-assembly of amyloidogenic proteins, including amyloid β -protein, tau, and α -synuclein. This small molecule interferes with aggregation by binding selectively to lysine side chains, changing the charge distribution of aggregation-prone proteins and thereby disrupting aggregate formation. However, the effects of CLR01 in cardiomyocytes undergoing proteotoxic stress have not been explored. Here we assess whether CLR01 can decrease cardiac protein aggregation catalyzed by cardiomyocyte-specific expression of mutated α B-crystallin (CryAB^{R120G}).

Methods and Results—A proteotoxic model of desmin-related cardiomyopathy caused by cardiomyocyte-specific expression of CryAB^{R120G} was used to test the efficacy of CLR01 therapy in the heart. Neonatal rat cardiomyocytes were infected with adenovirus expressing either wild-type CryAB or CryAB^{R120G}. Subsequently, the cells were treated with different doses of CLR01 or a closely related but inactive derivative, CLR03. CLR01 decreased aggregate accumulation and attenuated cytotoxicity caused by CryAB^{R120G} expression in a dose-dependent manner, whereas CLR03 had no effect. Ubiquitin-proteasome system function was analyzed using a ubiquitin-proteasome system reporter protein consisting of a short degron, CL1, fused to the COOH-terminus of green fluorescent protein. CLR01 improved proteasomal function in CryAB^{R120G} cardiomyocytes but did not alter autophagic flux. In vivo, CLR01 administration also resulted in reduced protein aggregates in CryAB^{R120G} transgenic mice.

Conclusions—CLR01 can inhibit CryAB^{R120G} aggregate formation and decrease cytotoxicity in cardiomyocytes undergoing proteotoxic stress, presumably through clearance of the misfolded protein via increased proteasomal function. CLR01 or related compounds may be therapeutically useful in treating the pathogenic sequelae resulting from proteotoxic heart disease. (*J Am Heart Assoc.* 2017;6:e006182. DOI: 10.1161/JAHA.117.006182.)

Key Words: amyloid • animal model cardiovascular disease • cardiomyopathy • chaperones • proteasome

Protein quality control (PQC) is pivotal to cellular homeostasis and integrity.¹ The loss or imbalance of protein homeostasis (proteostasis) leads to the accumulation of misfolded proteins and protein aggregates with consequent proteotoxicity and proteinopathy.^{2,3} These accumulations

have been implicated in numerous pathologies, including cardiovascular disease, neurodegenerative disease, diabetes mellitus, and cancer.^{1,4} For example, misfolded proteins that can form aggregates and toxic, preamyloid oligomers have been observed in diseased human hearts resulting from either hypertrophic or idiopathic dilated cardiomyopathy.⁵ These preamyloid oligomers can cause cardiac failure.⁶ Therapeutic approaches that focus on decreasing misfolded protein concentrations may be effective in decreasing morbidity and improving long-term outcomes. Because cardiomyocytes are postmitotic and are not rapidly replaced, maintaining balanced proteostasis is fundamental in minimizing cellular dysfunction and death.¹ Therefore, it is important to find effective therapeutic approaches for the cardiac proteinopathies.

Proteostasis is maintained by balancing multiple cellular pathways, including protein synthesis, quality control functions, and degradation, which participate in every aspect of cardiac physiology and pathology.³ The ubiquitin-proteasome

From the Division of Molecular Cardiovascular Biology, the Heart Institute, Cincinnati Children's Hospital, Cincinnati, OH (N.X., H.O., J.R.); Department of Neurology, David Geffen School of Medicine, Brain Research Institute, and Molecular Biology Institute, University of California at Los Angeles, CA (G.B.); Faculty of Chemistry, University of Duisburg-Essen, Essen, Germany (T.S., F.-G.K.).

Correspondence to: Jeffrey Robbins, PhD, Division of Molecular Cardiovascular Biology, The Heart Institute, Cincinnati Children's Hospital, 240 Sabin Way, MLC7020, Cincinnati, OH 45229-3039. E-mail: jeff.robbs@cchmc.org
Received March 23, 2017; accepted June 21, 2017.

© 2017 The Authors. Published on behalf of the American Heart Association, Inc., by Wiley. This is an open access article under the terms of the Creative Commons Attribution-NonCommercial-NoDerivs License, which permits use and distribution in any medium, provided the original work is properly cited, the use is non-commercial and no modifications or adaptations are made.

Clinical Perspective

What Is New?

- A “molecular tweezer’s” efficacy in relieving cardiac proteotoxicity was tested in a well-defined model of desmin-related cardiomyopathy.
- Proof of principle is presented that the molecular tweezer is effective in preventing aggregate load under proteotoxic conditions.
- The prevalent mechanism of this prevention appears to be upregulation of proteasomal activity.

What Are the Clinical Implications?

- Cardiovascular disease can be caused by and is often accompanied by alterations in protein homeostasis and the accumulation of aggregated proteins.
- Small molecules known as molecular tweezers can decrease proteotoxic load and prevent or ameliorate aggregate formation, showing proof of principle as a potential therapeutic agent.

system (UPS) and the autophagy-lysosome pathway are the major proteolytic processes for eliminating misfolded proteins, large aggregates, and damaged organelles. PQC insufficiency can result in misfolded or damaged proteins undergoing aberrant aggregation, which can then further impair the PQC in a vicious cycle. The main strategies guarding against these pathogenic events include upregulating molecular chaperones to fold or refold misfolded proteins and enhancing UPS or autophagy-lysosome pathway activity to remove the misfolded or damaged proteins.^{7,8}

Our current understanding of proteinopathy is based partially on studies of mutant proteins that are aggregation-prone. Desmin-related myopathy is a striated muscle disease that can present as skeletal muscle weakness and cardiomyopathy.^{9,10} It is characterized by intracellular protein aggregation, mitochondrial deficiencies, proteasomal dysfunction, and cell apoptosis in skeletal and cardiac myocytes.^{11–13} Mutations in a number of different genes encoding desmin, α B-crystallin (CryAB), and myotilin can cause this disease.¹⁴ Among these mutations, a missense mutation, R120G, in CryAB (CryAB^{R120G}) has been intensively studied. Either mouse or human CryAB^{R120G} expression in mouse cardiomyocytes resulted in aberrant protein aggregation and cardiomyopathy, recapitulating key features of human desmin-related cardiomyopathy.^{15–17} Abundant formation of aberrant granulofilamentous aggregates containing CryAB and CryAB^{R120G}, desmin, and other proteins occurred, and soluble, preamyloid oligomers and perinuclear concentrations of aggregates were present.^{5,16} Similar structures are characteristic of multiple neurodegenerative diseases as a result of amyloid β -protein (A β), α -synuclein,

mutant polyglutamine, or prion aggregation.^{14,18} We and others have shown that restoring normal PQC activity by augmenting chaperone production or upregulating the UPS or autophagy-lysosome pathway systems can result in reduced protein aggregate levels and decreased toxic preamyloid oligomers in cardiomyocytes, thereby decreasing morbidity and prolonging survival of CryAB^{R120G} mice.^{18–20}

The molecular tweezer CLR01 is a broad-spectrum nanochaperone that inhibits abnormal protein self-assembly by binding selectively to lysine residues, preventing aggregation and decreasing the toxicity of multiple amyloidogenic proteins.^{21,22} Selective binding to lysine is achieved by a combination of hydrophobic and electrostatic interactions, which are important in aberrant protein self-assembly.²³ Thus, CLR01 competes for the same sites that are key to nucleation and aggregation by most amyloidogenic proteins, including A β , tau, α -synuclein, islet amyloid polypeptide, and transthyretin.^{23–28} CLR01 has been tested in several in vitro and in vivo models of amyloidoses for inhibiting protein aggregation without signs of toxicity.²⁹ Considering the commonalities between CryAB^{R120G} and the amyloidogenic diseases, we wished to test whether CLR01 had therapeutic effects in CryAB^{R120G} cardiomyopathy. Our study revealed that CLR01 significantly inhibited CryAB^{R120G}-induced protein aggregate formation and decreased proteotoxicity in cardiomyocytes.

Methods

Molecular Tweezers

CLR01 and CLR03 were prepared and purified as sodium salts as described previously.³⁰

Animals

Transgenic mice with cardiomyocyte-restricted overexpression of either normal CryAB (CryAB^{WT}) or CryAB^{R120G} were used in this study.¹⁶ CLR01 was injected subcutaneously at different doses of 1, 3, or 6 mg/kg daily for 5 weeks beginning at 4 weeks after birth. Animals were handled in accordance with the principles and procedures of the *Guide for the Care and Use of Laboratory Animals*. The Institutional Animal Care and Use Committee at Cincinnati Children’s Hospital approved all experimental procedures.

Neonatal Rat Ventricular Myocytes and Adenovirus Infection

Primary neonatal rat ventricular myocytes (NRVMs) were isolated from the ventricles of 1- to 2-day-old Sprague-Dawley rats and plated at a density of 1×10^5 cells in a 2-well

chamber slide or 1.5×10^6 in 10-cm dishes in 10% fetal bovine serum in DMEM (Life Technologies, Carlsbad, CA). Twenty-four hours after plating, cells were infected with adenovirus (Ad) containing wild-type or the mutant CryAB tagged with green fluorescent protein (AdGFP-CryAB^{WT} or AdGFP-CryAB^{R120G}, respectively) for 2 hours in DMEM without fetal bovine serum, and then replaced with DMEM with 2% fetal bovine serum and $1 \times$ penicillin/streptomycin. Cells were subsequently treated with CLR01 or CLR03 at doses of 0.1, 1, 10, or 100 $\mu\text{mol/L}$. Four days later, cells were collected.

Measuring Proteasomal Activity and Autophagic Flux

NRVMs were coinfecting with adenoviruses containing Flag-CryAB^{R120G} and GFPu (an inverse reporter of the UPS) in serum-free DMEM for 2 hours. The medium was then changed to DMEM with 2% fetal bovine serum. Cells were subsequently treated with 100 $\mu\text{mol/L}$ CLR01 for 48 hours. Before collection, cells were treated with the proteasome inhibitor epoxomicin (Calbiochem, Darmstadt, Germany; 324801) at 250 nmol/L for 15 hours. Proteasome activity was then determined by quantitating fluorescence after immunostaining. In some experiments NRVMs were infected with AdGFP-CryAB^{R120G} and treated with 100 $\mu\text{mol/L}$ CLR01 for 48 hours. Before collection, cells were treated with Bafilomycin A1 (Sigma, St. Louis, MO; B1793) at 50 nmol/L for 3 hours in order to measure autophagic flux.²⁰ Cellular autophagy was then determined by quantitating LC3-II after Western blotting.

Cell Fractionation and Western Blot Analysis

NRVMs were briefly lysed in ice-cold CellLytic M buffer (Sigma, St. Louis, MO) containing a protease inhibitor mixture (Roche, Basel, Switzerland). The cells were then centrifuged at 12 000g for 15 minutes, and the supernatants collected (soluble fraction). The pellets were dissolved in DNase I (1 mg/mL in 10 mmol/L Tris, 15 mmol/L MgCl₂) (Roche), homogenized with a plastic pellet pestle, and gently sonicated. Protein concentration was measured with a modified Bradford assay. Both the soluble and insoluble proteins were then diluted with lysis buffer. For Western blot analysis, protein lysates were dissolved in $1 \times$ Laemmli buffer and heated at 99°C for 5 minutes. Proteins were then electrophoresed on SDS-PAGE and transferred to a polyvinylidene fluoride membrane (BioRad, Hercules, CA). Membranes were blocked for 1 hour in 5% nonfat dried milk and incubated with primary antibodies at 4°C overnight. Membranes were then washed with 0.1% Tween 20 in PBS, incubated with IRDye goat anti-mouse or anti-rabbit IgG secondary antibodies (LI-COR Biosciences, Lincoln, NE). The signal was detected with the Odyssey CLx Imaging System (LI-COR Biosciences). The following antibodies were used for

immunoblotting: anti-CryAB (1:2000, Enzo Life Sciences, Farmingdale, NY); anti-GAPDH (1:5000, EMD Millipore, Darmstadt, Germany); anti- β -actin (1:1000, Sigma, St. Louis, MO); anti-LC3 (1:1000, Cell Signaling Technology, Beverly, MA); anti-GFP (1:1000, Santa Cruz Biotechnology, Dallas, TX).

Immunofluorescence Microscopy

NRVMs were washed with PBS, fixed and then permeabilized with 4% paraformaldehyde and 0.5% Triton- \times 100 in PBS for 15 minutes. After being washed with PBS twice, fixed cells were incubated with 0.1 mol/L citrate buffer (pH 6.0) for 20 minutes. Subsequently, cells were blocked with iTFX signal enhancer (Molecular Probes, Eugene, OR) for 30 minutes and blocking buffer (1% BSA, 0.1% Tween 20 in PBS) for 1 hour at room temperature. Cells were then incubated with primary antibodies diluted in blocking buffer at 4°C overnight. Cells were washed and incubated with secondary antibodies conjugated to Alexa Fluor (Molecular Probes, Eugene, OR) for 1 hour at room temperature. DAPI at a 1:5000 dilution in PBS was used to stain the nuclei for 5 minutes. Cells were then washed with PBS and mounted using Vectashield Hard Set mounting medium (Vector BioLabs, Malvern, PA). Cells were analyzed using an A1R confocal microscope (Nikon, Tokyo, Japan). Relative aggregate areas per cell were quantitated using NIS-elements software (Nikon) with the observer blinded as to sample identity. Primary antibodies used were: anti-Troponin I (1:1000, EMD Millipore, Darmstadt, Germany); anti-CryAB (1:500, Enzo Life Sciences, Farmingdale, NY); anti-cardiac myosin binding protein C (1:500, Abcam, Cambridge, UK).

Cellular Toxicity Assay

Lactate dehydrogenase activity in the collected cell medium was measured using a cytotoxicity detection kit (Roche, Basel, Switzerland) following the manufacturer's protocols.

Statistical Analysis

All parameters are presented as mean \pm SEM. Data were analyzed using 2-tailed Student t test between 2 groups. For multiple comparisons, ANOVA with post hoc testing was used. A value of $P < 0.05$ was considered statistically significant.

Results

CLR01 Protects Against CryAB^{R120G}-Induced Cytotoxicity

Misfolded proteins that aggregate can be proteotoxic and lead to cardiomyocyte death.³¹ We infected neonatal NRVMs with adenovirus containing either wild-type CryAB or CryAB^{R120G}.

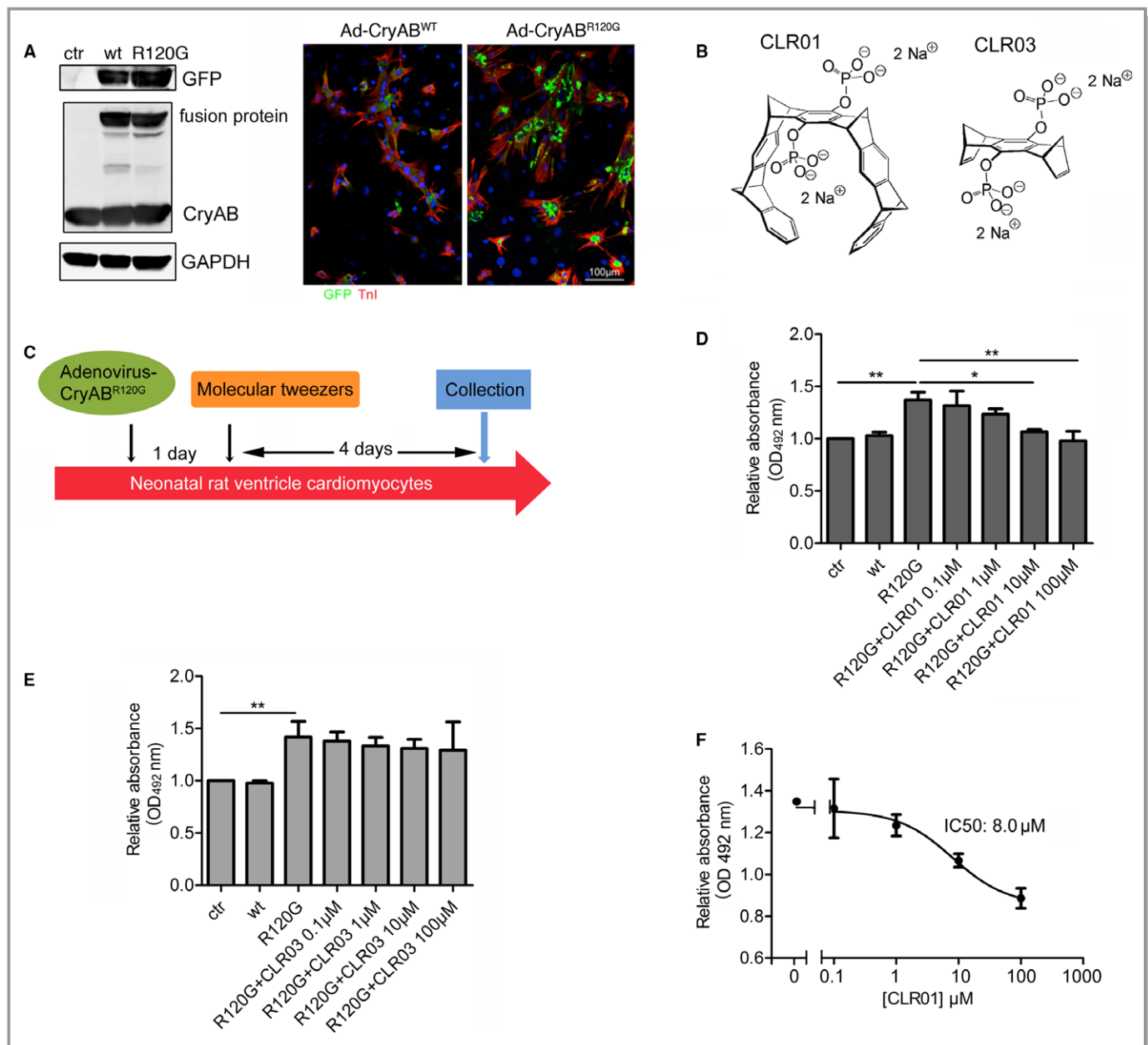


Figure 1. A, Aggregates are formed in neonatal rat ventricular cardiomyocytes infected with R120G adenovirus. Cells were infected with either AdGFP-CryAB^{WT} or AdGFP-CryAB^{R120G} (adenovirus constructs containing green fluorescent protein tags (GFP) linked to the α B crystallin (CryAB) normal or mutant constructs (AdGFP-CryAB^{WT} or AdGFP-CryAB^{R120G}, respectively) at a multiplicity of infection of 10. Five days later, cells were fixed and immunostained with troponin I to identify cardiomyocytes and DAPI to label the nuclei. Both the CryAB-fusion GFP proteins (fusion) and CryAB protein are easily detectable with equal amounts of adenovirus-driven CryAB and CryAB^{R120G} present. B, The experimental strategy. The structures of CLR01 and CLR03 are shown, and (C) the experiment is schematically outlined. D, CLR01 protects against R120G-induced cytotoxicity. Increasing doses of CLR01 led to decreased cytotoxicity. E, CLR03 was expected to be ineffective at preventing aggregation and to serve as a negative control. CLR03 treatment had no effect on R120G-induced cytotoxicity. F, Dose-response curve for CLR01 inhibition of R120G-induced cytotoxicity. $n=7$ for all samples used. The IC₅₀ value is indicated. ctr; non-infected cells, wt indicates AdGFP-CryAB^{WT}; R120G, AdGFP-CryAB^{R120G}. * $P<0.05$, ** $P<0.01$.

As expected, overexpression of wild-type CryAB, driven by AdGFP-CryAB^{WT} infection showed diffuse GFP distribution in the NRVMs, but AdGFP-CryAB^{R120G}-infected cells showed large, GFP-positive aggregates after 5 days (Figure 1A). To examine whether CLR01 can decrease the proteotoxicity

caused by CryAB^{R120G} cardiomyocyte expression, we first designed an in vitro cell-based experimental strategy using the NRVMs (Figure 1B and C). The ability of CLR01 as well as a closely related but inactive molecule, CLR03, to decrease overall cell toxicity was tested using the lactate

dehydrogenase cell toxicity assay (Methods) (Figure 1D and E). By 5 days postinfection, CryAB^{R120G} expression caused significant proteotoxicity. CLR01 treatment alleviated CryAB^{R120G}-induced cytotoxicity in a dose-dependent manner, whereas CLR03 had no effect. The IC₅₀ of CLR01 was 8.0 μmol/L (Figure 1F), a value that is well within the range reported for inhibition of other amyloid or amyloidogenic proteins.²⁴ We conclude that CLR01 at relatively high concentrations is protective against CryAB^{R120G}-induced cytotoxicity.

CLR01 Inhibits CryAB^{R120G}-Induced Protein Aggregation

Because cytotoxicity in the CryAB^{R120G} model is a function of accumulating aggregate load, we asked whether CLR01 treatment reduced aggregate levels. Adenovirus-infected NRVMs were treated with different doses of CLR01 or CLR03 starting at 24 hours after infection. Five days later, aggregates were quantitated (Figure 2A and B). The data show decreasing aggregate loads with increasing CLR01 concentrations and that CLR03 had no effect at any dose used (Figure 2C and D). The IC₅₀ of CLR01 was 7.8 μmol/L (Figure 2E).

The immunostaining results showed that CLR01 treatment at a concentration of >1 μmol/L significantly reduced protein aggregates. To confirm that insoluble, misfolded protein levels were not simply disbursed throughout the cytoplasm but still present, we analyzed the soluble and insoluble protein fractions (Methods) from the CLR01- and CLR03-treated infected cells, subjecting the fractions to gel electrophoresis and Western analyses with CryAB antibody.

We used 100 μmol/L CLR01 or CLR03 treatment to quantitate insoluble and soluble CryAB levels (Figure 3). CLR01 dramatically reduced the amount of CryAB present in the insoluble protein fraction (Figure 3A), whereas CLR03 did not have a significant effect (Figure 3B). Soluble CryAB levels were largely restored to normal levels in the CLR01-treated cells but not in the CLR03-treated cultures (Figure 3C and D). Together, the data show that CLR01 potently decreases aggregate load and accumulation of insoluble CryAB in the proteotoxic cardiac environment produced by CryAB^{R120G} expression and can restore wild-type levels of the normal, soluble protein.

CLR01 Blocks CryAB^{R120G}-Induced Aggregate Formation

To determine whether CLR01 acted by inhibiting aggregate formation or by clearing preexisting aggregates, 100 μmol/L CLR01 was added at either 1 day or 3 days post-AdGFP-CryAB^{R120G} infection for 48 hours. Cells were fixed and

stained daily. Under normal culture conditions, aggregates gradually accumulate over the 5-day period post-AdGFP-CryAB^{R120G} infection (Figure 4A, column 1). When CLR01 was added at 1 day postinfection for 48 hours, visible aggregates were only rarely present 2 to 5 days postinfection, and accumulation was significantly slowed relative to the untreated control cells (Figure 4A, compare column 1 with column 2). When CLR01 was added at 3 days postinfection for 48 hours, a time when aggregates have already accumulated, aggregate levels remained static but did not decrease over the next 48 hours (Figure 4A and B). Our findings suggest that CLR01 affects cardiac protein aggregation by inhibiting aggregate formation rather than by clearing preexisting aggregates.

CLR01 Enhances Ubiquitin-Proteasome Activity

Cardiac UPS function is severely impaired by CryAB^{R120G} expression, which amplifies the effects of defective protein turnover and protein aggregation.³² Considering CLR01's effects on preventing initial formation of the aggregates, we reasoned that it might be affecting the UPS. We used the inverse reporter protein GFPu to study the level of UPS activity.¹⁹ GFPu is efficiently degraded by the UPS, and changes in GFPu protein levels reflect UPS proteolytic function, with high levels indicating poor UPS function. As expected on the basis of prior data,³² GFP levels were elevated in NRVMs infected with AdFlagCryAB^{R120G} (Figure 5A), indicating impaired UPS activity. Treatment with 100 μmol/L CLR01 significantly decreased GFP in both noninfected and AdFlag-CryAB^{R120G}-infected conditions (Figure 5A and B). NRVMs were also treated for 15 hours with 250 nmol/L epoxomicin, a proteasome inhibitor, confirming the system's utility. CLR01 treatment was unable to reverse epoxomicin inhibition of proteasomal activity under noninfected conditions. However, CLR01 did decrease GFP accumulation in epoxomicin-treated CryAB^{R120G}-expressing cardiomyocytes (Figure 5).

CLR01 Treatment Does Not Alter Autophagic Flux

We subsequently studied whether CLR01 had an effect on another major proteolytic pathway, autophagy. We hypothesized that it would have minimal effect on this pathway because autophagy is involved predominantly in the clearance of preexisting aggregates.^{20,33} We have documented that autophagy is compromised in the CryAB^{R120G} hearts and that upregulated autophagy effectively reduced protein aggregate loads, leading to increased cell viability, conserved cardiac function, and increased probability of survival.^{20,33} Consistent with the proteasomal data (Figure 5) showing that CLR01's actions appear to be focused on aggregate accretion rather

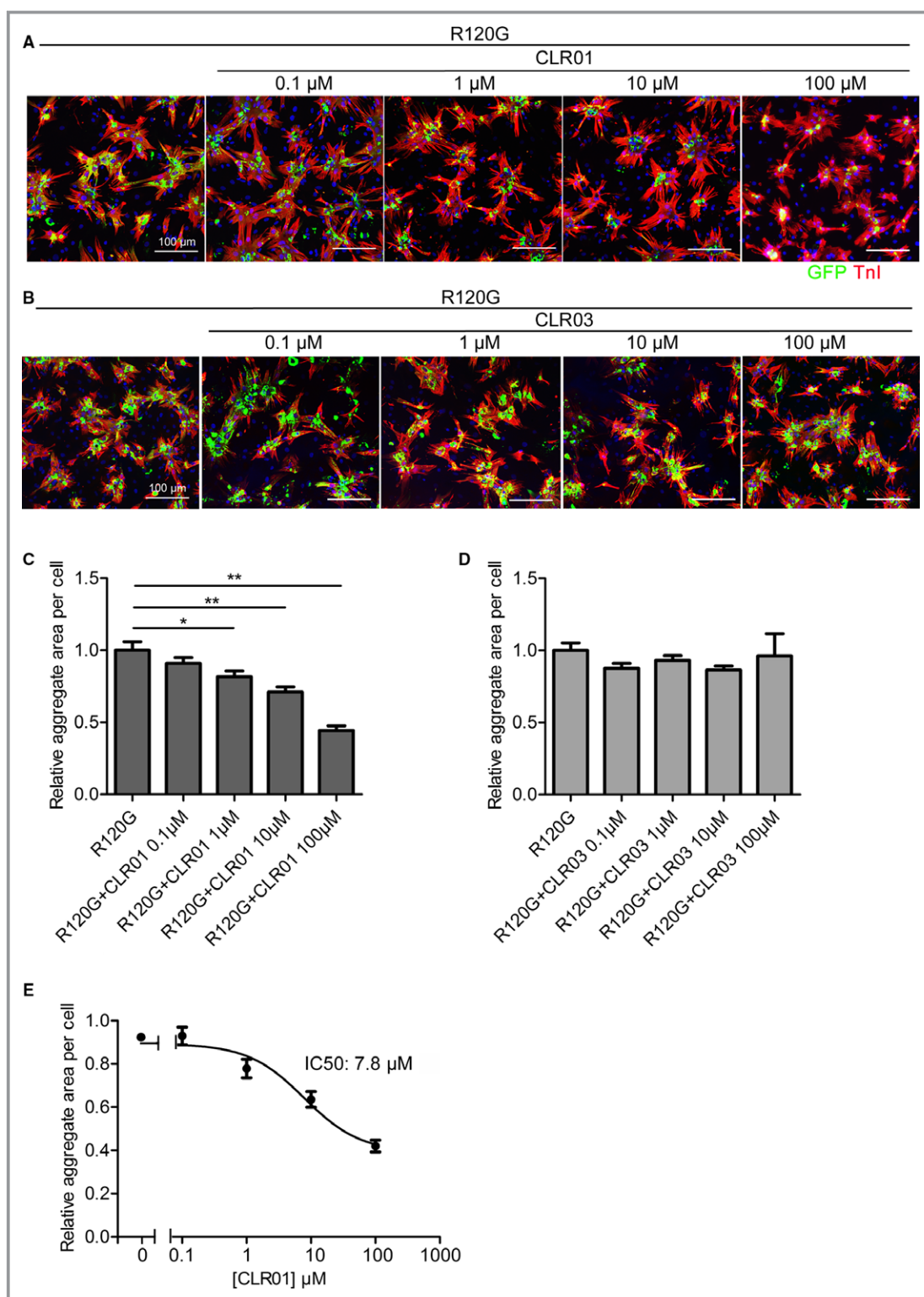


Figure 2. CLOR1 inhibits R120G-induced protein aggregation in a dose-dependent manner. Neonatal rat ventricular cardiomyocytes were infected with AdGFP-CryAB^{R120G} and treated with different doses of CLOR1 or CLOR3. A and B, NRVMs were fixed and immunostained with troponin I (TnI; red) and 4',6-diamidino-2-phenylindole (DAPI, nuclear staining; blue). C and D, Aggregates (green) in the neonatal rat ventricular cardiomyocytes were quantitated using NIS-elements (Nikon) software. E, Dose-response curve for CLOR1 inhibition of R120G-induced protein aggregation. At least 100 cells were quantitated in each group for each experiment, and each group was replicated n=6. The IC₅₀ value is indicated. R120G indicates AdGFP-CryAB^{R120G}. * P <0.05, ** P <0.01.

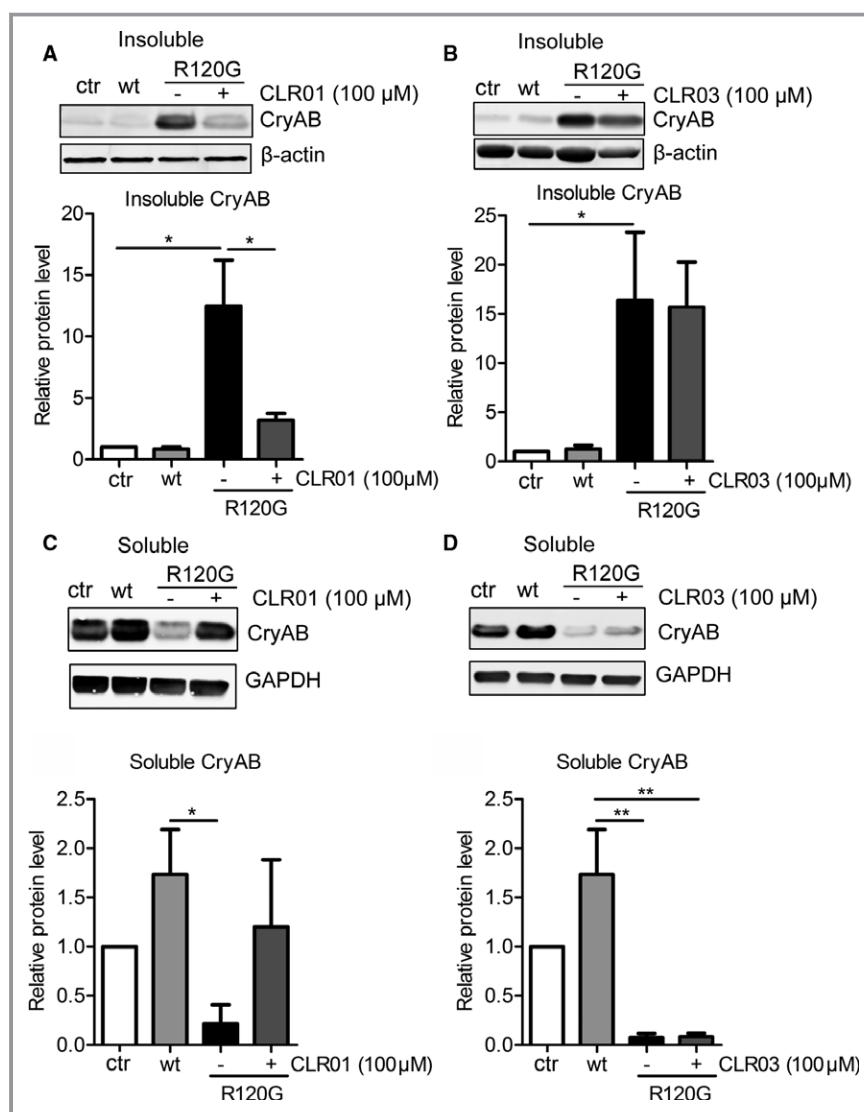


Figure 3. CLR01 decreases insoluble CryAB. A and B, Sample Western blots and insoluble CryAB quantitation. β -Actin was used as a loading control. $*P < 0.05$. C and D, Sample Western blot analysis of soluble CryAB. Glyceraldehyde 3-phosphate dehydrogenase (GAPDH) was as a loading control. Ctr indicates noninfected cells; wt, AdGFP-CryAB^{WT}; R120G, AdGFP-CryAB^{R120G}. The quantitations of the Western blots are shown immediately below their respective blots. $*P < 0.05$, $**P < 0.001$. Experiments were each performed in triplicate.

than clearance, NRVM autophagic flux was unaffected by 100 μ mol/L CLR01. Levels of the autophagic marker LC3-II were unchanged, and autophagic flux, as measured by the addition of Bafilomycin A1 (Methods), was also unaffected (Figure 6A and B).

CLR01 Administration Reduces Aggregate Accumulation in CryAB^{R120G} Hearts

Based on the in vitro data showing that CLR01 inhibited CryAB^{R120G}-induced protein aggregation, we wished to determine if CLR01 could decrease aggregate formation in the intact

heart as well. Four-week-old CryAB^{R120G} mice were injected subcutaneously with CLR01 at 1, 3, and 6 mg/kg on a daily basis for an additional 5 weeks (Figure 7A). At 4 weeks, visible aggregates are just beginning to form but increase rapidly during the ensuing 5-week period (Figure 7A, bottom panels). Although some hypertrophy is present (Figure 7), gross cardiac organization and overall anatomy and performance are unaffected at this relatively early time.^{16,20} After 5 weeks of CLR01 dosing, the mice were euthanatized, and the hearts examined for aggregate accumulation using immunohistochemistry to detect CryAB. Heart-weight-to-body-weight ratios were not statistically affected by the 5-week drug regimen (Figure 7B),

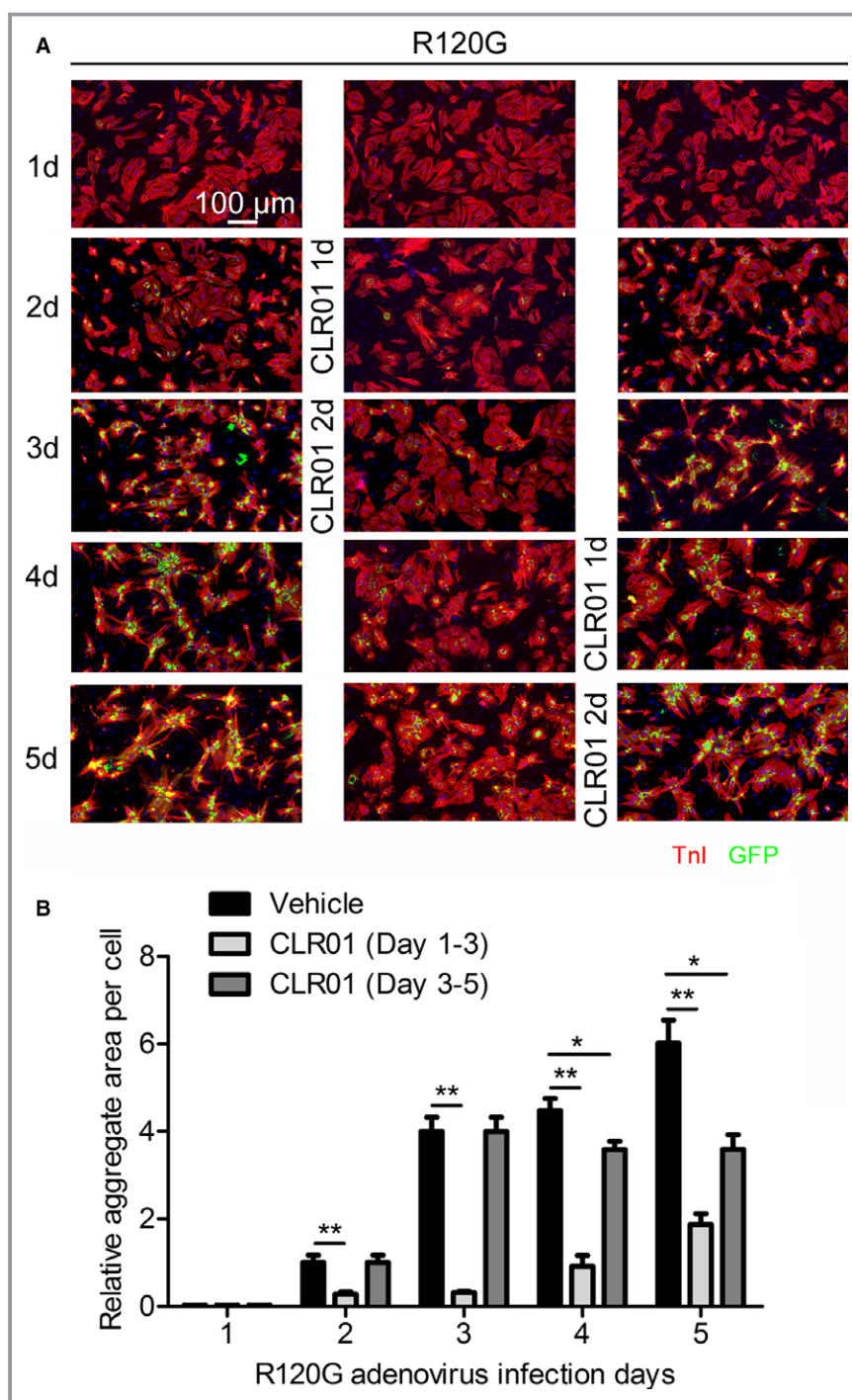


Figure 4. CLR01 blocks R120G-induced aggregate formation. A, Neonatal rat ventricular cardiomyocytes were fixed and immunostained with TnI and DAPI at different days after AdGFP-CryAB^{R120G} infection. Column 1 contains cells that were untreated with CLR01. CLR01 was added at either 1 day (column 2) or 3 days postinfection (column 3) in order to explore its effects on formation vs clearance of aggregates. B, Aggregates were quantitated using NIS-elements software. R120G indicates AdGFP-CryAB^{R120G}. At least 100 cells were quantitated in each group for each experiment, and each group was replicated with n=6. * $P<0.05$, ** $P<0.01$.

although there was a slight downward trend in the heart-weight-to-body-weight ratio. However, CryAB-positive aggregate areas decreased in a dose-dependent manner and were

significantly smaller at a dose of 6 mg/kg per day as compared with the lower doses used (Figure 7C and D). Consistent with these data, we looked at the very sensitive molecular markers

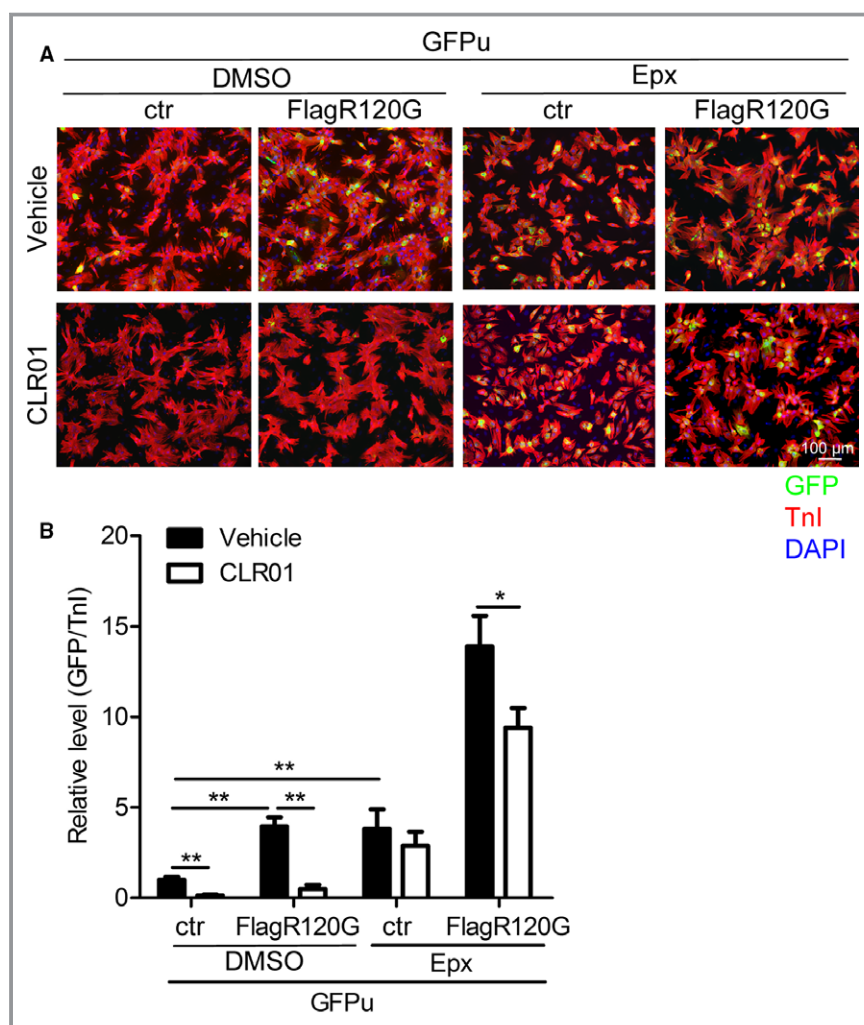


Figure 5. CLRO1-treated neonatal rat ventricular cardiomyocytes show enhanced ubiquitin-proteasome activity. The cardiomyocytes were coinfecting with a proteasome activity reporter, an adenoviral vector expressing an inverse reporter of the ubiquitin-proteasome system; Ad-GFPu (ctr), and AdFlag-R120G (FlagR120G). Cells were subsequently treated with CLRO1 (100 μ mol/L) for 48 hours and the proteasomal inhibitor epoxomicin (Epx) for 15 hours. A, Three days after adenovirus infection, cells were fixed and immunostained with TnI and DAPI. B, Quantification of the relative GFP level in cardiomyocytes using NIS-elements software. Quantification of the relative GFP level in cardiomyocytes was done with NIS-elements. $n=6$ * $P<0.05$, ** $P<0.01$.

for cardiac hypertrophy or stress, the atrial and brain natriuretic peptides. The transcripts for both factors were significantly elevated, as expected, in the CryAB^{R120G} hearts, and 5 weeks of CLRO1 treatment resulted in significantly decreased levels of both atrial and brain natriuretic peptide transcripts (Figure 7E and F).

Discussion

Data that can help us understand the genetic basis of proteinopathies, including desmin-related cardiomyopathy, continue to accumulate but have not yet resulted in any

effective therapy for this type of heart disease. By utilizing both cell culture and the CryAB^{R120G} mouse model, we were able to show that the molecular tweezer CLRO1 can inhibit CryAB^{R120G}-induced aggregate formation and ameliorate proteotoxicity in cardiomyocytes.

CLRO1 is a novel, selective, and broad-spectrum inhibitor of aberrant protein self-assembly, acting by a process-specific mechanism and inhibiting the aggregation and toxicity of multiple amyloidogenic proteins, including A β , tau, and α -synuclein, at different concentrations.^{24,34} CLRO1 was originally developed as an artificial lysine receptor^{30,35} that binds lysine residues with low micromolar affinity. It also binds to arginine with ~ 10 -fold lower affinity. CLRO1 acts as a

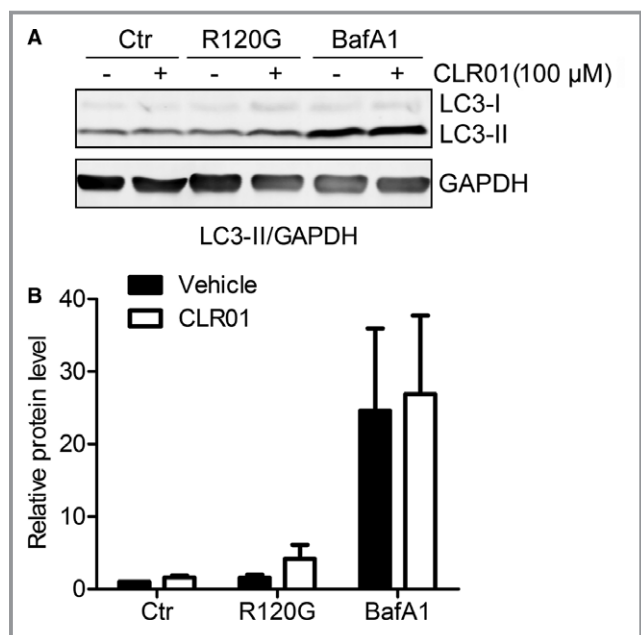


Figure 6. Neonatal rat ventricular cardiomyocytes autophagic flux is not affected by CLR01 treatment. Cells were infected with AdGFP-CryAB^{R120G} for 3 days or treated with the lysosomal inhibitor Bafilomycin A1 (BafA1) at 50 nmol/L for 3 hours. Cells were treated with or without CLR01 for 48 hours. A, A sample Western blot showing the levels of microtubule-associated protein 1A/1B-light chain 3 (LC3-I) and its phosphatidylethanolamine conjugate (LC3-2). GAPDH was used as a loading control. B, The Western blot was quantitated. ctr indicates noninfected cells; R120G, AdGFP-CryAB^{R120G}. The experiment was performed in triplicate.

nanochaperone using selective binding to lysine by a combination of hydrophobic and electrostatic interactions, which are important in aberrant protein self-assembly.^{21,29} CLR01 suppressed α -synuclein fibril assembly and disaggregated preformed fibrils in neurons, rescuing the animal's neurodegenerative phenotype and promoting survival in zebrafish embryos expressing human α -synuclein³⁴ or treated with the Parkinson disease-linked pesticide Ziram.³⁶ Similarly, it reduced α -synuclein accumulation and aggregation and promoted neuron survival in a lamprey model of spinal-cord injury.³⁷ CLR01 also was able to inhibit A β fibrillogenesis and cleared existing A β and tau aggregates in the brain of an Alzheimer disease model in mice.³⁸ The compound also decreased transthyretin aggregation in familial amyloidotic polyneuropathy,³⁹ and inhibited islet amyloid polypeptide aggregation and toxicity in rat insulinoma cells.^{25,40}

We treated NRVMs with CLR01 or CLR03 at concentrations ranging from 0.1 to 100 μ mol/L. A concentration of 10 μ mol/L CLR01 was protective in a CryAB^{R120G}-induced cytotoxicity cellular environment, but the inactive molecular tweezer derivative CLR03 had no effect. At a relatively high concentration of 100 μ mol/L for both CLR01 and the inactive CLR03, we

observed no cytotoxicity, but CLR01 was quite effective in ameliorating proteotoxicity and inhibited the formation of visible aggregates by \approx 50% with an IC₅₀ of 8.0 μ mol/L (Figure 2). When added at the time of CryAB^{R120G} infection, 100 μ mol/L CLR01 almost completely prevented aggregate formation. These levels are well within the effective ranges observed for the aggregation properties of multiple amyloidogenic proteins when they were subjected to CLR01 treatment.²⁴

There are numerous data pointing to the safety of high doses of CLR01 both in vitro and in vivo. CLR01 increased PC-12 cell viability relative to control cells at concentrations up to 200 μ mol/L and inhibited α -synuclein assembly in the presence of a 10-fold molar excess of CLR01.^{24,34} The moderate binding affinity of CLR01 for lysine residues suggests that highly labile binding can still effectively interfere with the weak molecular interactions that lead to formation of toxic oligomers.²² Aggregation-prone proteins could thus remain soluble, allowing them to be degraded by the normal cellular clearance mechanisms, as has been demonstrated for α -synuclein.³⁴

These mechanisms underlying CLR01's beneficial effects in inhibiting abnormal accumulation of protein aggregates led us to hypothesize that it might also be therapeutically effective in CryAB^{R120G}-mediated proteotoxicity, brought about as a result of the mutant crystallin's expression in cardiomyocytes.³⁴ CLR01 indeed inhibited CryAB^{R120G} aggregation and cytotoxicity efficiently in cultured cardiomyocytes. In vivo, CLR01 administered at a relatively early age, when aggregates are just beginning to form in CryAB^{R120G} cardiomyocytes, appears to be therapeutically useful in preventing protein aggregation. CLR01 decreased cardiac proteotoxic aggregate formation in the intact animal, and the dose used did not result in any detectable cardiac abnormalities or hypertrophy. Previously, daily injection of doses up to 10 mg/kg did not produce any signs of toxicity in mice.²⁹ Our study provides a safe and efficient dose for decreasing aggregate formation in the mouse heart. These initial in vivo results have prompted us to begin to design more comprehensive animal studies with larger cohorts who will receive the drug at different times during aggregate development to understand the full spectrum of CLR01 in this particular model.

Misfolded proteins pose a major threat to cell homeostasis if they are not refolded by molecular chaperones or removed by the clearance mechanisms. They can not only form nonfunctional aggregates, but also recruit and inactivate other essential proteins.⁴¹ In the PQC network that maintains proteostasis the UPS is considered the most significant degradation mechanism. An impaired UPS affects the cell's ability to remove damaged or misfolded proteins,¹⁹ and can lead to increased misfolded protein loads and large, proteinaceous aggregates. In CryAB^{R120G}-expressing cells the UPS is severely impaired.¹ Our finding that CLR01 treatment

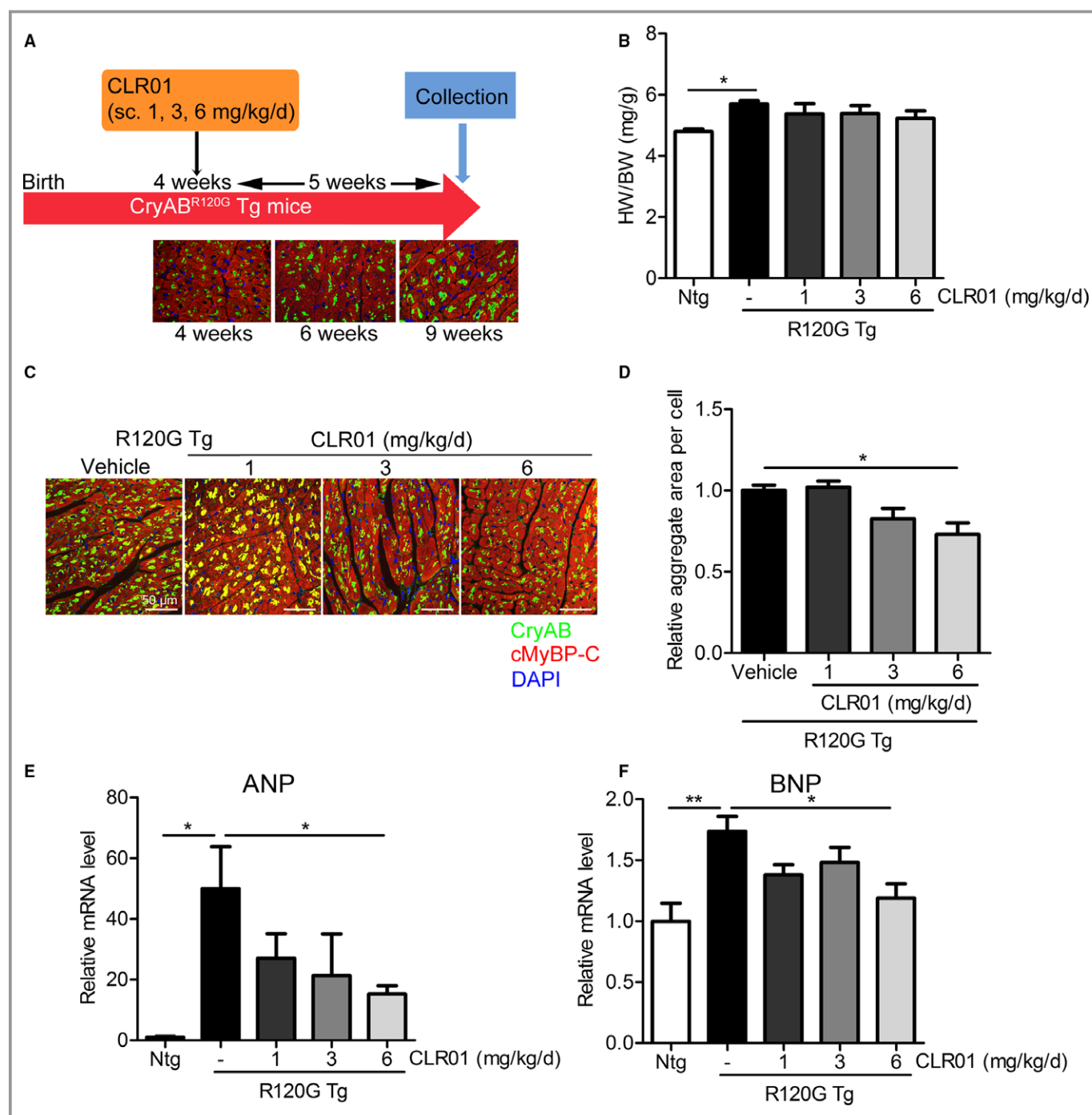


Figure 7. CLR01 administration reduces aggregate content in CryAB^{R120G} mice. **A**, A schematic diagram showing the experimental strategy. Four-week-old CryAB^{R120G} mice were subcutaneously injected with either vehicle or CLR01 (1, 3, 6 mg/kg daily) for 5 weeks, and the hearts were collected. At least 4 mice were used in each group. Also shown are the aggregate levels present at the times indicated. Magnifications are the same as in **C**. **B**, Heart-weight-to-body-weight ratios at 9 weeks. **C**, Representative images showing aggregates in the hearts. Immunofluorescent staining was carried out with CryAB (alpha B crystallin) antibody (green) to identify aggregates and cardiac myosin binding protein C (cardiac myosin binding protein C) antibody (red) to identify cardiomyocytes. The nuclei were counterstained with DAPI (blue). Calibration bars are 50 μ m. **D**, Quantification of the aggregates using NIS-elements software. **E** and **F**, Transcript levels for both atrial natriuretic protein (ANP) and brain natriuretic peptide (BNP) were determined by reverse transcribed polymerase chain reaction. * P <0.05, ** P <0.01. Tg indicates transgenic.

significantly enhanced cardiomyocyte UPS activity is consistent with previous studies showing that CLR01 alleviated UPS inhibition caused by α -synuclein overexpression.³⁴

Autophagy is another critical pathway for degrading large aggregates of misfolded proteins and damaged organelles.² Compromised autophagy is linked to the development of

different pathologies, including heart failure and some neurodegenerative diseases.^{42,43} During the process of aberrant protein aggregation, the UPS and autophagy may both be compromised.^{2,31,42,43} Although CLR01 blocked CryAB^{R120G} aggregate formation, we saw no changes in autophagic flux, implying that CLR01's effects are mediated through its initial efficacy in blocking aggregate formation rather than clearance of preexisting aggregates through autophagy.

In summary, we show here that CLR01 inhibits CryAB^{R120G} aggregate formation both in vitro and in vivo. CLR01 ameliorates CryAB^{R120G}-induced proteotoxicity and restores UPS activity in cardiomyocytes. Our findings support further development of CLR01 for treating proteotoxic heart disease.

Sources of Funding

This work was supported by NIH grants P01HL69779, P01HL059408, R01HL05924, R01HL062927, a Trans-Atlantic Network of Excellence grant from Le Fondation Leducq (Robbins), and by the UCLA Mary S. Easton Endowment (Bitan).

Disclosures

None.

References

- Wang ZV, Hill JA. Protein quality control and metabolism: bidirectional control in the heart. *Cell Metab*. 2015;21:215–226.
- Willis MS, Patterson C. Proteotoxicity and cardiac dysfunction—Alzheimer's disease of the heart? *N Engl J Med*. 2013;368:455–464.
- Lim J, Yue Z. Neuronal aggregates: formation, clearance, and spreading. *Dev Cell*. 2015;32:491–501.
- Kim YE, Hipp MS, Bracher A, Hayer-Hartl M, Hartl FU. Molecular chaperone functions in protein folding and proteostasis. *Annu Rev Biochem*. 2013;82:323–355.
- Sanbe A, Osinska H, Saffitz JE, Glabe CG, Kaye R, Maloyan A, Robbins J. Desmin-related cardiomyopathy in transgenic mice: a cardiac amyloidosis. *Proc Natl Acad Sci USA*. 2004;101:10132–10136.
- Pattison JS, Sanbe A, Maloyan A, Osinska H, Klevitsky R, Robbins J. Cardiomyocyte expression of a polyglutamine preamyloid oligomer causes heart failure. *Circulation*. 2008;117:2743–2751.
- Tyedmers J, Mogk A, Bukau B. Cellular strategies for controlling protein aggregation. *Nat Rev Mol Cell Biol*. 2010;11:777–788.
- Rochet JC. Novel therapeutic strategies for the treatment of protein-misfolding diseases. *Expert Rev Mol Med*. 2007;9:1–34.
- Goldfarb LG, Park KY, Cervenakova L, Gorokhova S, Lee HS, Vasconcelos O, Nagle JW, Semino-Mora C, Sivakumar K, Dalakas MC. Missense mutations in desmin associated with familial cardiac and skeletal myopathy. *Nat Genet*. 1998;19:402–403.
- Dalakas MC, Park KY, Semino-Mora C, Lee HS, Sivakumar K, Goldfarb LG. Desmin myopathy, a skeletal myopathy with cardiomyopathy caused by mutations in the desmin gene. *N Engl J Med*. 2000;342:770–780.
- Maloyan A, Osinska H, Lammerding J, Lee RT, Cingolani OH, Kass DA, Lorenz JN, Robbins J. Biochemical and mechanical dysfunction in a mouse model of desmin-related myopathy. *Circ Res*. 2009;104:1021–1028.
- Maloyan A, Sanbe A, Osinska H, Westfall M, Robinson D, Imahashi K, Murphy E, Robbins J. Mitochondrial dysfunction and apoptosis underlie the pathogenic process in α -B-crystallin desmin-related cardiomyopathy. *Circulation*. 2005;112:3451–3461.
- Kumarapeli AR, Horak K, Wang X. Protein quality control in protection against systolic overload cardiomyopathy: the long term role of small heat shock proteins. *Am J Transl Res*. 2010;2:390–401.
- McLendon PM, Robbins J. Desmin-related cardiomyopathy: an unfolding story. *Am J Physiol Heart Circ Physiol*. 2011;301:H1220–H1228.
- Vicart P, Caron A, Guicheney P, Li Z, Prevost MC, Faure A, Chateau D, Chapon F, Tome F, Dupret JM, Paulin D, Fardeau M. A missense mutation in the α B-crystallin chaperone gene causes a desmin-related myopathy. *Nat Genet*. 1998;20:92–95.
- Wang X, Osinska H, Klevitsky R, Gerdes AM, Nieman M, Lorenz J, Hewett T, Robbins J. Expression of R120G- α B-crystallin causes aberrant desmin and α B-crystallin aggregation and cardiomyopathy in mice. *Circ Res*. 2001;89:84–91.
- Rajasekaran NS, Connell P, Christians ES, Yan LJ, Taylor RP, Orosz A, Zhang XQ, Stevenson TJ, Peshock RM, Leopold JA, Barry WH, Loscalzo J, Odelberg SJ, Benjamin IJ. Human α B-crystallin mutation causes oxidative stress and protein aggregation cardiomyopathy in mice. *Cell*. 2007;130:427–439.
- Sanbe A, Yamauchi J, Miyamoto Y, Fujiwara Y, Murabe M, Tanoue A. Interruption of CryAB-amyloid oligomer formation by HSP22. *J Biol Chem*. 2007;282:555–563.
- Gupta MK, Gulick J, Liu R, Wang X, Molkentin JD, Robbins J. Sumo E2 enzyme UBC9 is required for efficient protein quality control in cardiomyocytes. *Circ Res*. 2014;115:721–729.
- Bhuiyan MS, Pattison JS, Osinska H, James J, Gulick J, McLendon PM, Hill JA, Sadoshima J, Robbins J. Enhanced autophagy ameliorates cardiac proteinopathy. *J Clin Invest*. 2013;123:5284–5297.
- Attar A, Bitan G. Disrupting self-assembly and toxicity of amyloidogenic protein oligomers by “molecular tweezers”—from the test tube to animal models. *Curr Pharm Des*. 2014;20:2469–2483.
- Schrader T, Bitan G, Klarner FG. Molecular tweezers for lysine and arginine—powerful inhibitors of pathologic protein aggregation. *Chem Commun (Camb)*. 2016;52:11318–11334.
- Sinha S, Lopes DH, Bitan G. A key role for lysine residues in amyloid β -protein folding, assembly, and toxicity. *ACS Chem Neurosci*. 2012;3:473–481.
- Sinha S, Lopes DH, Du Z, Pang ES, Shanmugam A, Lomakin A, Talbiersky P, Tennstaedt A, McDaniel K, Bakshi R, Kuo PY, Ehrmann M, Benedek GB, Loo JA, Klarner FG, Schrader T, Wang C, Bitan G. Lysine-specific molecular tweezers are broad-spectrum inhibitors of assembly and toxicity of amyloid proteins. *J Am Chem Soc*. 2011;133:16958–16969.
- Lopes DH, Attar A, Nair G, Hayden EY, Du Z, McDaniel K, Dutt S, Bravo-Rodriguez K, Mittal S, Klarner FG, Wang C, Sanchez-Garcia E, Schrader T, Bitan G. Molecular tweezers inhibit islet amyloid polypeptide assembly and toxicity by a new mechanism. *ACS Chem Biol*. 2015;10:1555–1569.
- Zheng X, Liu D, Klarner FG, Schrader T, Bitan G, Bowers MT. Amyloid β -protein assembly: the effect of molecular tweezers CLR01 and CLR03. *J Phys Chem B*. 2015;119:4831–4841.
- Lump E, Castellano LM, Meier C, Seeliger J, Erwin N, Sperlich B, Sturzel CM, Usmani S, Hammond RM, von Einem J, Gerold G, Kreppel F, Bravo-Rodriguez K, Pietschmann T, Holmes VM, Palesch D, Zirafi O, Weissman D, Sowislok A, Wettig B, Heid C, Kirchhoff F, Weil T, Klarner FG, Schrader T, Bitan G, Sanchez-Garcia E, Winter R, Shorter J, Munch J. A molecular tweezer antagonizes seminal amyloids and HIV infection. *Elife*. 2015;4. pii: e05397. doi: 10.7554/eLife.05397
- Acharya S, Safaie BM, Wongkongkathep P, Ivanova MI, Attar A, Klarner FG, Schrader T, Loo JA, Bitan G, Lapidus LJ. Molecular basis for preventing α -synuclein aggregation by a molecular tweezer. *J Biol Chem*. 2014;289:10727–10737.
- Attar A, Chan WT, Klarner FG, Schrader T, Bitan G. Safety and pharmacological characterization of the molecular tweezer CLR01—a broad-spectrum inhibitor of amyloid proteins' toxicity. *BMC Pharmacol Toxicol*. 2014;15:23.
- Talbiersky P, Bastkowski F, Klarner FG, Schrader T. Molecular clip and tweezer introduce new mechanisms of enzyme inhibition. *J Am Chem Soc*. 2008;130:9824–9828.
- McLendon PM, Robbins J. Proteotoxicity and cardiac dysfunction. *Circ Res*. 2015;116:1863–1882.
- Chen Q, Liu JB, Horak KM, Zheng H, Kumarapeli AR, Li J, Li F, Gerdes AM, Wawrousek EF, Wang X. Intracellular amyloidosis impairs proteolytic function of proteasomes in cardiomyocytes by compromising substrate uptake. *Circ Res*. 2005;97:1018–1026.
- Pattison JS, Osinska H, Robbins J. Atg7 induces basal autophagy and rescues autophagic deficiency in CryAB^{R120G} cardiomyocytes. *Circ Res*. 2011;109:151–160.
- Prabhudesai S, Sinha S, Attar A, Kotagiri A, Fitzmaurice AG, Lakshmanan R, Ivanova MI, Loo JA, Klarner FG, Schrader T, Stahl M, Bitan G, Bronstein JM. A novel “molecular tweezer” inhibitor of α -synuclein neurotoxicity in vitro and in vivo. *Neurotherapeutics*. 2012;9:464–476.

35. Fokkens M, Schrader T, Klarner FG. A molecular tweezer for lysine and arginine. *J Am Chem Soc*. 2005;127:14415–14421.
36. Lulla A, Barnhill L, Bitan G, Ivanova MI, Nguyen B, O'Donnell K, Stahl MC, Yamashiro C, Klarner FG, Schrader T, Sagasti A, Bronstein JM. Neurotoxicity of the Parkinson disease-associated pesticide ziram is synuclein-dependent in zebrafish embryos. *Environ Health Perspect*. 2016;124:1766–1775.
37. Fogerson SM, van Brummen AJ, Busch DJ, Allen SR, Roychaudhuri R, Banks SM, Klarner FG, Schrader T, Bitan G, Morgan JR. Reducing synuclein accumulation improves neuronal survival after spinal cord injury. *Exp Neurol*. 2016;278:105–115.
38. Attar A, Ripoli C, Riccardi E, Maiti P, Li Puma DD, Liu T, Hayes J, Jones MR, Lichti-Kaiser K, Yang F, Gale GD, Tseng CH, Tan M, Xie CW, Straudinger JL, Klarner FG, Schrader T, Frautschy SA, Grassi C, Bitan G. Protection of primary neurons and mouse brain from Alzheimer's pathology by molecular tweezers. *Brain*. 2012;135:3735–3748.
39. Ferreira N, Pereira-Henriques A, Attar A, Klarner FG, Schrader T, Bitan G, Gales L, Saraiva MJ, Almeida MR. Molecular tweezers targeting transthyretin amyloidosis. *Neurotherapeutics*. 2014;11:450–461.
40. Attar A, Rahimi F, Bitan G. Modulators of amyloid protein aggregation and toxicity: EGCG and CLR01. *Transl Neurosci*. 2013;4:385–409.
41. Lee JG, Takahama S, Zhang G, Tomarev SI, Ye Y. Unconventional secretion of misfolded proteins promotes adaptation to proteasome dysfunction in mammalian cells. *Nat Cell Biol*. 2016;18:765–776.
42. Ravikumar B, Vacher C, Berger Z, Davies JE, Luo S, Oroz LG, Scaravilli F, Easton DF, Duden R, O'Kane CJ, Rubinsztein DC. Inhibition of mTOR induces autophagy and reduces toxicity of polyglutamine expansions in fly and mouse models of Huntington disease. *Nat Genet*. 2004;36:585–595.
43. Kassiotis C, Ballal K, Wellnitz K, Vela D, Gong M, Salazar R, Frazier OH, Taegtmeyer H. Markers of autophagy are downregulated in failing human heart after mechanical unloading. *Circulation*. 2009;120:S191–S197.

Inhibition of Mutant α B Crystallin–Induced Protein Aggregation by a Molecular Tweezer

Na Xu, Gal Bitan, Thomas Schrader, Frank-Gerrit Klärner, Hanna Osinska and Jeffrey Robbins

J Am Heart Assoc. 2017;6:e006182; originally published August 8, 2017;

doi: 10.1161/JAHA.117.006182

The *Journal of the American Heart Association* is published by the American Heart Association, 7272 Greenville Avenue, Dallas, TX 75231

Online ISSN: 2047-9980

The online version of this article, along with updated information and services, is located on the World Wide Web at:

<http://jaha.ahajournals.org/content/6/8/e006182>